

Supplementary Materials for Control of Neuronal Growth Cone Navigation by Asymmetric Inositol 1,4,5-Trisphosphate Signals

Hiroki Akiyama, Toru Matsu-ura, Katsuhiko Mikoshiba, Hiroyuki Kamiguchi*

*To whom correspondence should be addressed. E-mail: kamiguchi@brain.riken.jp

Published 14 July 2009, *Sci. Signal.* **2**, ra34 (2009)

DOI: 10.1126/scisignal.2000196

This PDF file includes:

Materials and Methods

Fig. S1. IP₃R distribution in chick DRG growth cones.

Fig. S2. NGF gradients elicit asymmetric IP₃ signals in growth cones grown on laminin.

Fig. S3. Global Ca²⁺ signals in the growth cone triggered by photolysis of caged IP₃.

Fig. S4. Global Ca²⁺ signals triggered by PLC activation in the growth cone.

Fig. S5. Time course of changes in the spatial distribution of reagents ejected from a micropipette.

References

Supplementary Materials

Materials and Methods

Immunocytochemistry

DRG neurons were pre-loaded by trituration with an aldehyde-fixable analog of dextran that was conjugated with Alexa Fluor 594 (100 μ M, 10,000 MW, Invitrogen) and fixed at 37°C for 30 min in a solution consisting of: 80 mM Na-PIPES (pH 6.9), 1 mM $MgCl_2$, 1 mM EGTA, 3% sucrose, 0.1% glutaraldehyde and 4% formaldehyde. After washing with PBS, neurons were permeabilized and blocked with 0.1% Triton X-100 and 10% goat serum for 60 min, then incubated with 1 μ g/ml 4C11 anti-Type 1 IP_3R monoclonal antibody (1) overnight at 4°C. Primary antibody binding was visualized with Alexa Fluor 488-conjugated secondary antibody (10 μ g/ml, Invitrogen). Fluorescence images were acquired with a CCD-camera (ORCA-ERG with binning set at 2 x 2, Hamamatsu Photonics) mounted on an inverted microscope (IX81) with a 100x objective (UPlanSApo). To correct for differences in thickness within a growth cone, the fluorescence image of Alexa Fluor 488 was divided by that of Alexa Fluor 594.

Ca^{2+} imaging and global photolysis of caged IP_3 in the growth cone

DRG neurons were loaded with caged IP_3 and two Ca^{2+} indicators, OGB-1-AM (2 μ M, Invitrogen) and FR-AM (2.5 μ M, Invitrogen). Ca^{2+} imaging was performed using an inverted microscope (IX81) and a 100x objective (UPlanSApo). For simultaneous OGB-1/FR imaging, both indicators were excited with 492/18 nm light, and images were acquired every 1 sec with a CCD-camera (EM-CCD with binning set at 4 x 4) after splitting the dual-color image using an emission splitter (Dual-View) comprised of a 565 nm dichroic mirror, a 530/35 nm emission filter for OGB-1 and a 610-nm emission filter for FR. OGB-1/FR emission ratio (R_{Ca}) was used as a measure of $[Ca^{2+}]_c$. Caged IP_3 was photolyzed by exposing a growth cone to UV light from a xenon lamp (330–385 nm in wave length, three 100-msec pulses each separated by a 1-sec interval). The size of UV-irradiation area (~ 10 μ m in diameter) was controlled by a pinhole placed in the light path. Time-course changes of $[Ca^{2+}]_c$ were expressed as $R_{Ca}/R_{Ca-base}$, where $R_{Ca-base}$ is the mean of the 11 consecutive R_{Ca} values before the onset of UV photolysis (-10.3 to -0.3 sec). The peak amplitude was defined as the mean of three consecutive $R_{Ca}/R_{Ca-base}$ values with the maximal $R_{Ca}/R_{Ca-base}$ in the middle.

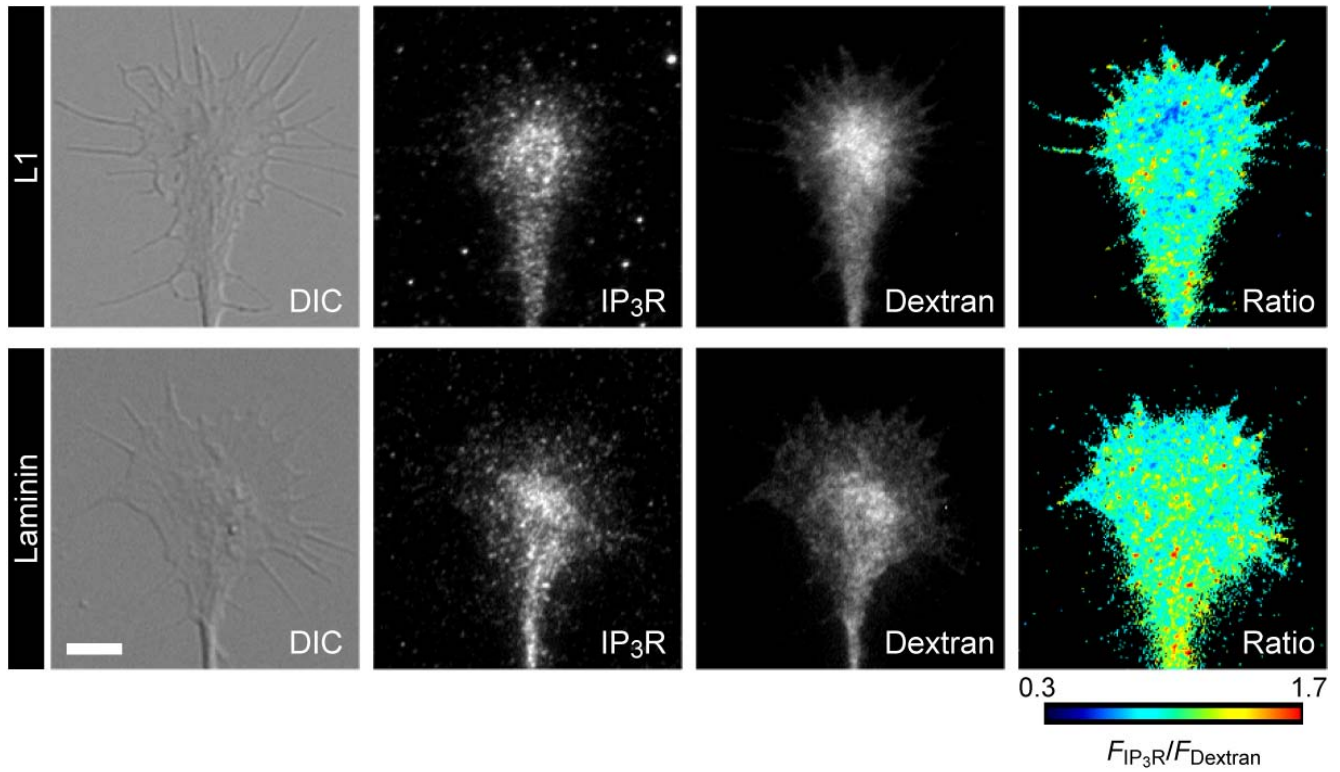


Fig. S1. IP₃R distribution in chick DRG growth cones. DRG neurons preloaded with Alexa Fluor-conjugated dextran were immunostained with the anti-IP₃R antibody 4C11. DIC images of the growth cone cultured on L1 (top) or laminin (bottom) are shown on the far left. Pseudo color images (far right) were obtained by dividing IP₃R immunofluorescence (middle left) by Alexa-dextran fluorescence (middle right). Ratio calculations were applied to Alexa-dextran-positive pixels. Scale bar, 5 μ m.

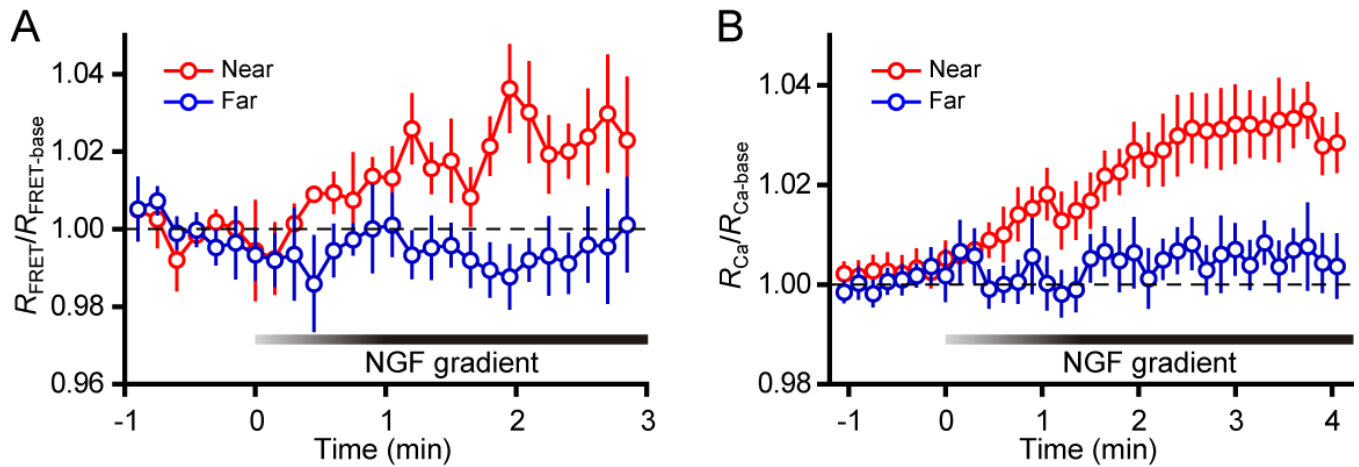


Fig. S2. NGF gradients elicit asymmetric IP₃ signals in growth cones grown on laminin. **(A)** Time-course of changes in [IP₃]_c, expressed as $R_{\text{FRET}}/R_{\text{FRET-base}}$ of IRIS-1, in the near (red circles) and far (blue circles) ROIs (n = 5 growth cones). **(B)** Time-course of changes in [Ca²⁺]_c, expressed as $R_{\text{Ca}}/R_{\text{Ca-base}}$, in the near (red circles) and far (blue circles) ROIs (n = 8 growth cones).

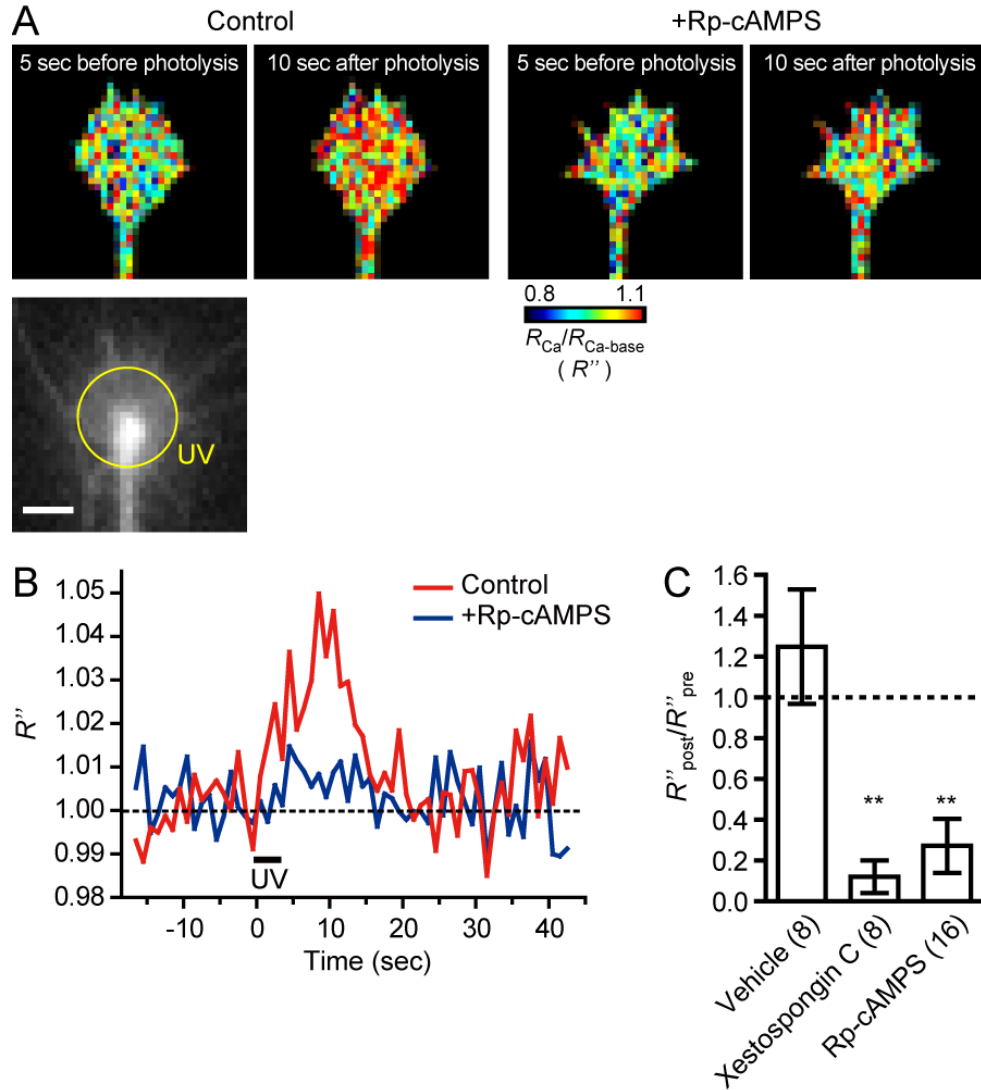


Fig. S3. Global Ca^{2+} signals in the growth cone triggered by photolysis of caged IP_3 . **(A)** A DRG growth cone on L1 loaded with caged IP_3 and two Ca^{2+} indicators, OGB-1 and FR. The grayscale image (bottom panel) shows FR fluorescence. The yellow circle represents the UV-irradiated area. The pseudo-color images represent $R_{Ca}/R_{Ca-base}$ (defined as R'') before and after UV photolysis. The same growth cone was analyzed before (control) and after (+Rp-cAMPS) 10-min treatment with Rp-cAMPS. Scale bar, 5 μm . **(B)** Time-course of changes in R'' averaged within the whole growth cone shown in (A), before (red line) and after (blue line) bath application of Rp-cAMPS. **(C)** The effect of the indicated drugs on the peak amplitude of increases in R'' induced by UV photolysis. R''_{pre}/R''_{post} represents drug-induced changes in amplitude of the Ca^{2+} signal. Numbers in parentheses indicate the number of growth cones examined. $**P < 0.01$ vs. vehicle, Dunnett's multiple comparison test.

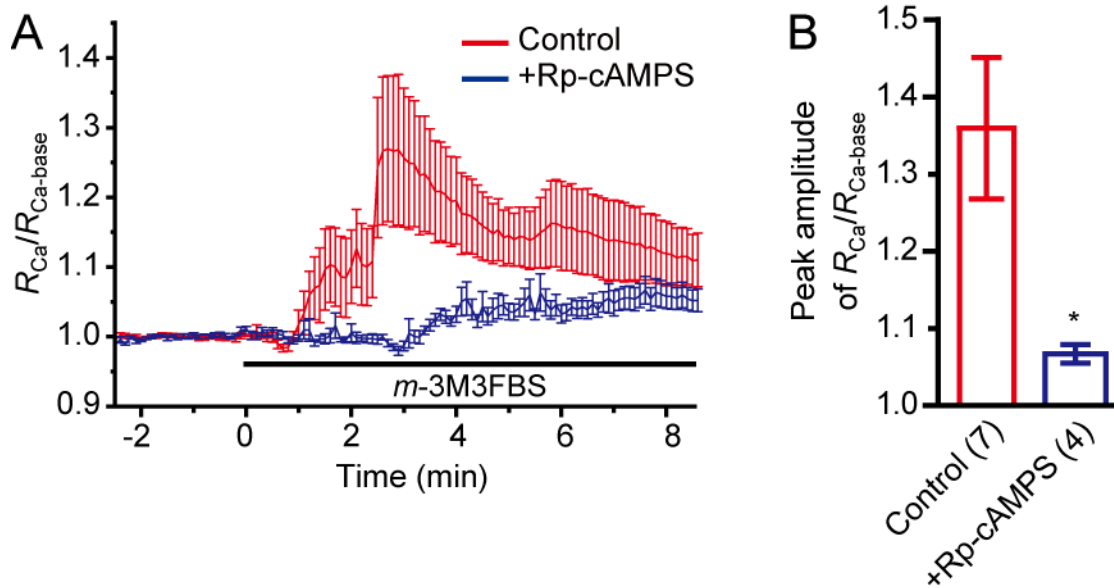


Fig. S4. Global Ca^{2+} signals triggered by PLC activation in the growth cone. **(A)** Growth cones on L1 were treated with 2,4,6-trimethyl-N-(*m*-3-trifluoromethylphenyl)benzenesulfonamide (*m*-3M3FBS; Calbiochem), which activates PLC and elicits PLC-dependent increases in $[Ca^{2+}]_c$ (2). The thick horizontal line indicates the presence of bath-applied *m*-3M3FBS (7 μ M). Images of OGB-1 and FR were simultaneously acquired every 6 sec, and $R_{Ca}/R_{Ca-base}$ averaged over the whole growth cone was plotted. Experiments were performed in the absence (red line) or presence (blue line) of Rp-cAMPS in bath media. **(B)** The peak amplitude of *m*-3M3FBS-induced $[Ca^{2+}]_c$ increases was compared in the absence (control) versus presence of Rp-cAMPS. Numbers in parentheses indicate the number of growth cones examined. * $P < 0.05$, unpaired t test.

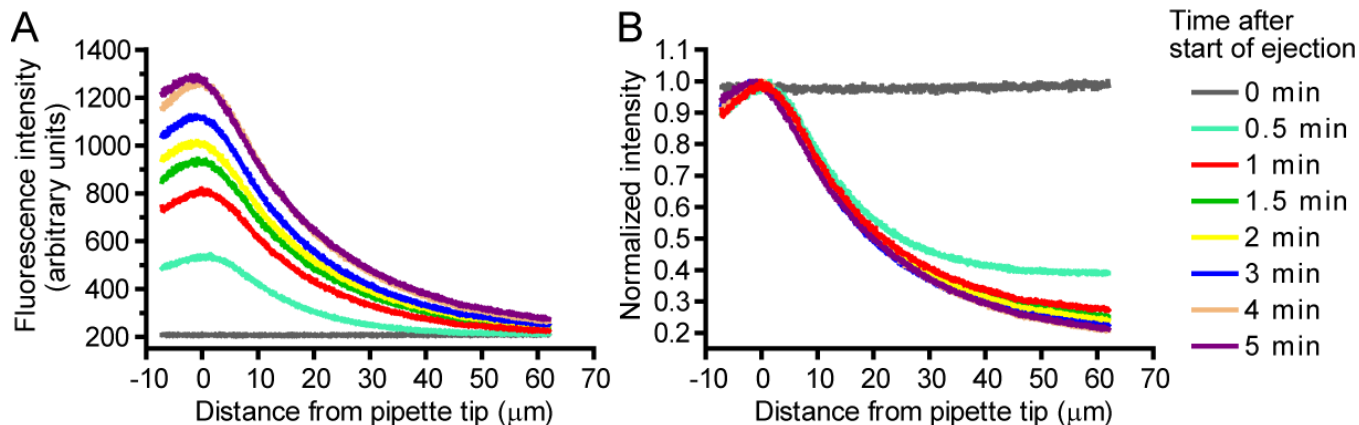


Fig. S5. Time-course of changes in the spatial distribution of reagents ejected from a micropipette. Rhodamine B (500 μM in pipette, Wako) was ejected into the medium by applying pulsatile pressure (4 psi in amplitude, 20 ms in duration, 2 Hz). Then, fluorescence images of rhodamine B were acquired using a 20x objective (UPlanSApo) on an inverted microscope (IX81) equipped with a CCD-camera (CoolSnap HQ with binning set at 2 x 2). **(A)** The fluorescence intensities of rhodamine B were plotted against the distance from the pipette tip. **(B)** The normalized intensities of rhodamine B fluorescence. The spatial distributions of normalized intensities during the period from 1 to 5 min after the start of ejection were statistically identical ($P = 1$, Kolmogorov-Smirnov test).

References

1. N. Maeda, M. Niinobe, Y. Inoue, K. Mikoshiba, Developmental expression and intracellular location of P400 protein characteristic of Purkinje cells in the mouse cerebellum. *Dev. Biol.* **133**, 67-76 (1989).
2. Y. S. Bae, T. G. Lee, J. C. Park, J. H. Hur, Y. Kim, K. Heo, J. Y. Kwak, P. G. Suh, S. H. Ryu, Identification of a compound that directly stimulates phospholipase C activity. *Mol. Pharmacol.* **63**, 1043-1050 (2003).